

Effect of radiative losses on the heat transfer from porous fins

Suhil Kiwan ^{*,1}

Mechanical Engineering Department, Jordan University of Science and Technology, PO Box 3030, Irbid, 11425, Jordan

Received 17 May 2006; received in revised form 23 August 2006; accepted 26 November 2006

Available online 13 March 2007

Abstract

The effect of radiation heat transfer on the natural convection heat transfer from a porous fin attached to a vertical isothermal surface has been investigated. The Rosseland approximation for the radiation heat exchange and the Darcy model for simulating the solid–fluid interactions in the porous medium have been adapted in this study. The governing equations are reduced to a single nonlinear ordinary differential equation. A closed form solution for the convection–radiation heat transfer from an infinite fin for low surface temperature parameter, θ_b , has been found and presented. The dimensionless temperature profiles, the effectiveness parameter, φBi , or the average Nusselt number are graphically displayed. The effect of varying Rayleigh number, Ra^* , the radiation–conduction parameter, Rd , the surface temperature parameter, θ_b , and the surface-ambient radiation parameter, R_2 , are presented. It is found that as the surface temperature parameters increases the radiation effect becomes important and as Ra^* increases the radiation effects become less important.

© 2006 Elsevier Masson SAS. All rights reserved.

Keywords: Porous fins; Natural convection; Heat transfer; Darcy model; Radiation losses; Rosseland approximation

1. Introduction

Reducing the size and cost of fins are the prime goals of fin industry. This requirement is often justified by the high cost of the high-thermal-conductivity metals that are employed in the manufacture of finned surfaces and by the cost associated with the weight of the fin especially in airplanes and motorcycles applications. These goals can be achieved by improving the heat transfer from fins. This improvement can be accomplished through the following techniques:

- (1) increasing the surface area to volume ratio,
- (2) increasing the thermal conductivity of the fin, and
- (3) increasing the heat transfer coefficients between the surface of the solid fin and the surrounding fluid.

Intensive studies have been performed to find the optimum shape of conventional fins. An overview of the fin optimum shaping issue has been presented by Snider and Kraus [1].

Poulikakos and Bejan [2] have shown that optimum fin shapes and dimensions can be determined also based on purely thermodynamic grounds. Shouman [3] found an exact general solution to the effect of radiation losses on the heat transfer from conventional solid fins.

Heat transfer in porous media has also gained a considerable attention of many researchers. Porous substrates of high thermal conductivity have been used to improve the thermal performance of different thermal systems [4]. Porous blocks have been used to control the flow and heat-transfer characteristics of an external surface [5]. Kiwan and Al-Nimr [6] numerically investigated the effect of using porous fins on the heat transfer from a heated horizontal surface. The basic philosophy behind using porous fins is to increase the effective area through which heat converted to ambient fluid. They found that using porous fin with certain porosity may give same performance as conventional fin and save 100 \tilde{e} of the fin material. More recently, Kiwan [7] developed a simple model to find the natural convection heat transfer from porous fin. Also, Kiwan and Zieton [8] numerically investigated the effect of using porous fins in the annulus between two concentrated cylinders. They found that using porous fins enhanced the heat transfer coefficient more than 70% compared to the use of conventional solid fins. Abu-

^{*} Tel.: +96614679798; fax: +96614676652.

E-mail addresses: kiwan@just.edu.jo, kiwan@ksu.edu.sa.

¹ On Leave at King Saud University, SA.

Nomenclature

A	cross sectional area
b	fin height
Bi	Biot number
C_F	Forchheimer number
c_p	specific heat
g	gravitational acceleration
k	thermal conductivity
k_r	thermal conductivity ratio, k_{eff}/k_f
K	permeability of the porous fin
L	fin length
\dot{m}	mass flow rate
P	fin perimeter
q	heat transfer rate
r	far-stream location from center of fin base
R_∞	dimensionless location of far-stream, r_∞/L
Rd	radiation–conduction parameter, $Rd = 4\sigma T_\infty^3/3\beta R k_{\text{eff}}$
R_2	surface-ambient radiation parameter, $R_2 = 4\sigma \varepsilon T_\infty^3 b/k_{\text{eff}}$
Ra^*	modified Rayleigh number, $\frac{g\beta(T_b - T_\infty)K}{\alpha v^2 k_r b}$
T	temperature at any point
T_b	temperature at the fin base
u	axial velocity
v	normal velocity
\bar{v}_w	average velocity of the fluid passing through the fin at any point
W	fin width
x	axial coordinate

X non-dimensional axial coordinate, x/b

Greek symbols

α	thermal diffusivity
β	thermal expansion coefficient
β_R	Rosseland extinction coefficient
ε	emissivity
$\tilde{\varepsilon}$	porosity
φ	fin effectiveness
ϕ	Angular displacement, Fig. 2
θ	dimensionless temperature
θ_b	surface temperature parameter, $\theta_b = T_b/T_\infty$
μ	dynamic viscosity
ν	kinematic viscosity
σ	Stefan–Boltzmann constant
ρ	density of the fluid

Subscripts

eff	effective properties
f	fluid
b	conditions at the fin base
s	solid
∞	ambient conditions
1	clear fluid domain
2	porous domain

Superscripts

$'$ derivative with respect to X

Hijleh [9] investigated numerically the effect of using porous fins on the natural convection heat transfer from a horizontal cylinder. He concluded that using porous fins provide much higher heat transfer rates than solid fins. However, he assumed that the fin thickness is very small ($t \rightarrow 0$) and it has a very high thermal conductivity (i.e., $k_r \rightarrow \infty$).

The experimental work in this area is very limited. Kim et al. [10] investigated experimentally the impact of using porous fins on the heat transfer and flow characteristics in plate fin heat exchanger. They found under certain conditions the porous fins give better heat transfer than louvered fins.

Thermal radiation plays an important role in situations where convection heat transfer coefficient is small and thus cannot be neglected. Ali et al. [11] studied the convection–radiation heat transfer by convection and radiation from a semi-infinite horizontal plate. They considered gray gas that emits and absorbs but does not scatter thermal radiation. Hossain and Takhar [12] investigated the effect of radiation on mixed convection flow of optically thick viscous and incompressible fluid over an isothermal vertical plate. They employed the Rosseland diffusion approximation. Hossain and Alim [13] analyzed the convection–conduction–radiation interaction in the natural convective flow along a thin vertical cylinder. They used local non-similarity method and the implicit finite difference scheme

with Keller box elimination method. Yih [14] has studied the effect of radiation on natural convection over an isothermal vertical cylinder embedded in a saturated porous medium using the modified Keller-box method to solve the resulted PDE where Darcy model is used to simulate the fluid flow in the porous medium. The effect of varying the radiation parameter ($Rd \sim 0.1–10$) on the heat transfer is presented. Cherif and Sifaoui [15] have considered radiation along with conduction and convection to predict the heat transfer behavior in a cylindrical enclosure. Badruddin et al. [16] studied the radiation effect on the natural convection heat transfer through a vertical annulus embedded in a porous medium. They presented the effect of radiation parameter ($Rd = 0–1$), aspect ratio and radius on the average Nusselt number and they found that the average Nusselt number increased significantly with increasing the radiation parameter. Hossain and Pop [17] studied the radiation effects on free convection over a vertical plate embedded in a porous medium with high porosity. They presented the effect of several parameters on the local skin friction and the local rate of heat transfer. It should be mentioned that references [13–17] deal with one fluid domain (i.e., porous domain) and they invoked the Local Thermal Equilibrium (LTE) assumption in writing the energy equation and they used Rosseland approximation to model the radiation heat transfer.

In the present work it is intended to develop a simple model which is able to analyze the effect of radiation losses on the natural convection heat transfer from porous fins. It is also anticipated to study the effect of operating and design parameters on the thermal performance of porous fins and compare the results with that obtained in available literature. It should be noted here that unlike Ref. [13–17] the present analysis assumes that heat transfer occurs within the porous media and between the porous media and the surroundings.

2. Analysis

Fig. 1 shows a simple rectangular fin attached to a vertical constant temperature wall. The cross-sectional area of the fin is constant. Being porous, the fin allows for the flow to infiltrate through it. In order to simplify the solution, the following assumptions are considered:

- (1) the porous medium is homogeneous, isotropic, and saturated with a single-phase fluid,
- (2) both the fluid and the solid matrix have constant physical properties except the density in the buoyancy term where Boussinesq approximation is used,
- (3) the temperature inside the fin is only function of x ,
- (4) the interactions between the porous medium and the clear fluid can be simulated by the Darcy formulation, and
- (5) following the work of [11–17] and in order to reduce the complexity of the problem the radiative heat flux inside the porous medium is assumed to behave as an optically thick gas.

It can be argued that if the gas filling the porous material is optically thick then the porous media containing this gas can be treated as optically thick. But if the gas is semi transparent or transparent then without experimental data and farther analysis on this issue it is difficult to decide how to treat a porous media

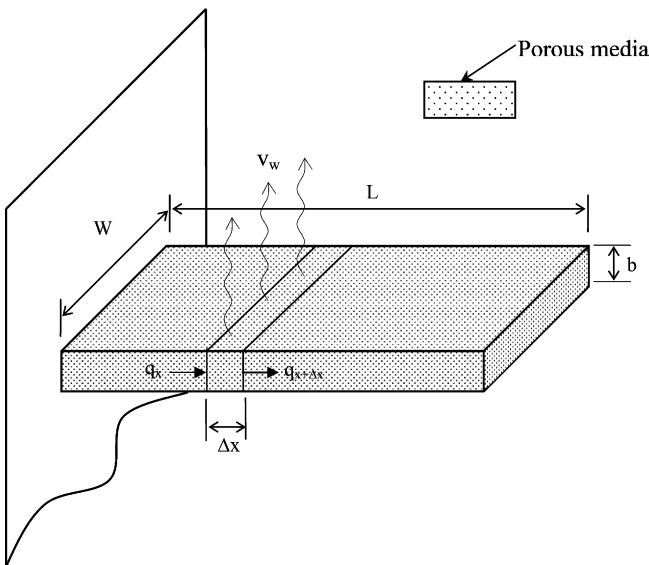


Fig. 1. Schematic diagram for the problem under consideration.

containing such gases. Therefore, this study is limited to porous medium that behave as optically thick gas.

The energy balance to the slice segment of the fin of thickness Δx , shown in Fig. 1, requires that

$$q(x) - q(x + \Delta x) = \dot{m}c_p(T(x) - T_\infty) + hP\Delta x(1 - \tilde{\varepsilon}) + P\Delta x\sigma\varepsilon\left(T^4(x) - \frac{\alpha}{\varepsilon}T_\infty^4\right) \quad (1)$$

The effect of radiation heat transfer appears in two terms of Eq. (1); the left-hand side which represents the net heat transfers from the base to the element by conduction and radiation and the last term on the right-hand side of Eq. (1) which represents the net exchange of heat by radiation between the porous fin and the surrounding at T_∞ . For the sake of simplicity it will be assumed that $\varepsilon = \alpha$. The first term on the right-hand side represents the amount of heat energy transferred by the fluid passing through the porous media. This fluid is induced by the buoyancy force created due to the temperature difference between the fin and the surroundings. In the limit when $\tilde{\varepsilon} \rightarrow 0$ and $K \rightarrow 0$ (i.e., $\dot{m} = 0$), Eq. (1) reduces to the classical solid fin problem with radiation effect reported by Ref. [3].

The mass flow rate of the fluid passing through the porous material can be written as,

$$\dot{m} = \rho\bar{v}_w\Delta x W \quad (2)$$

The value of \bar{v}_w should be estimated from the consideration of the flow in the porous medium. Referring to assumption (4) above, Dary's model gives,

$$\bar{v}_w(x) = \frac{gK\beta}{\nu}(T(x) - T_\infty) \quad (3)$$

The energy flux vector of combined radiation and conduction at the base of the fin can be expressed as:

$$q = q_{\text{conduction}} + q_{\text{radiation}} \quad (4)$$

where the conduction term can be expressed, using Fourier's law of conduction, as

$$q_{\text{conduction}} = -k_{\text{eff}}A_b \frac{dT}{dx} \quad (5)$$

and the radiation heat flux term is expressed by the Rosseland diffusion approximation proposed by Siegel and Howell [18] as

$$q_{\text{radiation}} = -\frac{4\sigma}{3\beta_R} \frac{dT^4}{dx} \quad (6)$$

The treatment of the radiation heat transfer for non-optically thick gases is more complicated and can be found in [18,19]. Substitution of Eqs. (4)–(6) into Eq. (1) gives,

$$\begin{aligned} & \frac{d}{dx} \left[\frac{dT}{dx} + \frac{4\sigma}{3\beta_R k_{\text{eff}}} \frac{dT^4}{dx} \right] \\ &= \frac{\rho c_p g K \beta}{b \nu k_{\text{eff}}} (T(x) - T_\infty)^2 + \frac{hP(1 - \tilde{\varepsilon})}{k_{\text{eff}} A_b} (T(x) - T_\infty) \\ &+ \frac{\sigma \varepsilon}{k_{\text{eff}} A_b} \frac{P}{(T^4(x) - T_\infty^4)} \end{aligned} \quad (7)$$

Eq. (7) represents a second order nonlinear ordinary differential equation. To solve this equation two boundary conditions are needed. The temperature at the base of the fin is T_b . Then

$$T(0) = T_b \quad (8)$$

The second boundary condition depends on the situation at the fin tip. Two cases are considered (1) infinitely long fin, (2) finite-length fin with insulated tip.

The rate of heat transferred from the fin is calculated at fin base as

$$q_b = -k_{\text{eff}} A_b \left(\frac{dT}{dx} \right)_{x=0} - \frac{4\sigma A_b}{3\beta_R} \left(\frac{dT^4}{dx} \right)_{x=0} \quad (9)$$

The following is the analysis for two cases considered in this study.

Case 1: Infinitely long fin with low θ_b .

In the situation where the temperature differences within the flow are assumed to be sufficiently small then the term T^4 may be expressed as a linear function of temperature

$$T^4 \cong 4T_\infty^3 T - 3T_\infty^4 \quad (10)$$

Introducing the non-dimensional temperature $\theta = \frac{T(x) - T_\infty}{T_b - T_\infty}$ and $X = \frac{x}{b}$ into Eq. (7) and using Eq. (10) yields

$$\theta''(1 + 4Rd) = Ra^* \theta^2 + \frac{Pb}{A_b} \left(\frac{h(1 - \tilde{\varepsilon})}{k_{\text{eff}}} + R_2 \right) \theta \quad (11)$$

where

$$Ra^* = \frac{g\beta(T_b - T_\infty)Kb}{\alpha\nu k_r}, \quad Rd = \frac{4\sigma T_\infty^3}{3\beta_R k_{\text{eff}}}, \quad R_2 = \frac{4\sigma \varepsilon T_\infty^3 b}{k_{\text{eff}}} \quad (12)$$

Multiplying Eq. (11) by θ' and then integrating the results noting that for infinitely long fin $\theta(X \rightarrow \infty) = 0$ and $\theta'(X \rightarrow \infty) = 0$, yields

$$\begin{aligned} \frac{d\theta}{dX} = - & \left[\frac{1}{(1 + 4Rd)} \left(\frac{2}{3} Ra^* \theta^3 \right. \right. \\ & \left. \left. + \frac{Pb}{A_b} \left(\frac{h(1 - \tilde{\varepsilon})}{k_{\text{eff}}} + R_2 \right) \theta^2 \right) \right]^{1/2} \end{aligned} \quad (13)$$

Apply Eq. (13) at $X = 0$ and noting that $\theta(0) = 1$, yields

$$\begin{aligned} \frac{d\theta}{dX} \Big|_{X=0} = - & \left[\frac{1}{(1 + 4Rd)} \left(\frac{2}{3} Ra^* \right. \right. \\ & \left. \left. + \frac{Pb}{A_b} \left(\frac{h(1 - \tilde{\varepsilon})}{k_{\text{eff}}} + R_2 \right) \right) \right]^{1/2} \end{aligned} \quad (14)$$

Defining fin effectiveness, φ , as the ratio of the rate of heat transfer from the fin, q_b , to the rate of heat transfer that would take place from the fin base area without the extended surface and without radiation effect, q_{bw} for the same temperature difference. The fin effectiveness can be written in terms of the dimensionless parameters defined earlier as;

$$\varphi = \frac{q_b}{q_{bw}} = \frac{-k_{\text{eff}}(1 + 4Rd)}{hb} \frac{d\theta}{dX} \Big|_{X=0}$$

and we can also define the average Nusselt number as

$$\begin{aligned} \overline{Nu} &= \frac{q_b}{k_{\text{eff}} A_b (T_b - T_\infty)} \\ &= -(1 + 4Rd) \frac{d\theta}{dX} \Big|_{X=0} = \frac{\varphi h b}{k_{\text{eff}}} \varphi Bi \\ &= - \left[(1 + 4Rd) \left(\frac{2}{3} Ra^* + \frac{Pb}{A_b} \left(\frac{h(1 - \tilde{\varepsilon})}{k_{\text{eff}}} + R_2 \right) \right) \right]^{1/2} \end{aligned} \quad (15)$$

To find the temperature distribution along the fin, integrate Eq. (13) and apply $\theta(0) = 1$, yields

$$X = \frac{1}{\sqrt{N}} \log \frac{(\sqrt{N + M\theta} - \sqrt{N})(\sqrt{N + M} + \sqrt{N})}{(\sqrt{N + M\theta} + \sqrt{N})(\sqrt{N + M} - \sqrt{N})} \quad (16)$$

where

$$\begin{aligned} M &= \frac{2Ra^*}{3(1 + 4Rd)} \quad \text{and} \\ N &= \frac{Pb}{A_b(1 + 4Rd)} \left(\frac{h(1 - \tilde{\varepsilon})}{k_{\text{eff}}} + R_2 \right) \end{aligned}$$

Eqs. (15) and (16) represent a closed form solution to the natural convection heat transfer from an infinite porous fin including radiation effects.

Case 2: Fins with any value of θ_b .

In the situations where θ_b is large then the approximation expressed by Eq. (10) is not valid. In this case, Eq. (7) can be manipulated to obtain

$$\begin{aligned} \theta''(1 + 4Rd\{\theta(\theta_b - 1) + 1\}^3) &= Ra^* \theta^2 - 12Rd(\theta_b - 1)\{\theta(\theta_b - 1) + 1\}^2 \theta'^2 \\ &+ \frac{R_2}{(\theta_b - 1) A_b} \frac{Pb}{A_b} ([(\theta_b - 1)\theta + 1]^4 - 1) \\ &+ \frac{h(1 - \tilde{\varepsilon})Pb}{k_{\text{eff}} A_b} \theta \end{aligned} \quad (17)$$

where $\theta_b = \frac{T_b}{T_\infty}$. The above equation is a second order nonlinear ODE subjected to the boundary conditions:

$$\begin{cases} \theta(0) = 1, \text{ and } \theta'(X \rightarrow \infty) = 0 & \text{infinite fin} \\ \theta(0) = 1, \text{ and } \theta'(X = L/b) = 0 & \text{insulated-tip fin} \end{cases} \quad (18)$$

And the heat transfer from the base of the fin can be expressed as

$$\overline{Nu} = \frac{q_b b}{k_{\text{eff}} A_b (T_b - T_\infty)} = -(1 + 4Rd \theta_b^3) \theta'(0) = \varphi Bi \quad (19)$$

3. Numerical solution procedure

The nonlinear differential equations given by Eq. (17) along with the relevant boundary conditions are solved using a variable order and variable step size finite difference method with deferred corrections. The solution method is based on the sub-program of Pereyra [20]. The first step in the solution is to reduce the governing equations to a system of first order differential equations. The basic discretization of the first order differential equations is the trapezoidal rule over a non-uniform

mesh. This mesh is chosen adaptively, to make the local error approximately the same size everywhere. Global error estimates are produced to control the computation. The resulting nonlinear algebraic system is solved by Newton's method with step control. The linearized system of equations is solved by Gauss elimination.

To verify the validity and the accuracy of the present analysis, results of the average Nusselt numbers were compared to those of previous investigations. The results of the similar analysis were compared with that obtained by Kiwan and Al-Nimr [6] and reported in [7]. The results showed an agreement within 10%. On the other hand, The value of \bar{Nu} for the natural convection in a vertical plate embedded in a porous media is 0.888 [21] while Eq. (15) gives $\bar{Nu} = 0.8165$. Badruddin et al. [16] showed that when $Rd = 0.33$, the value of $\bar{Nu} = 2.741$ while Eq. (15) gives $\bar{Nu} = 2.91$. These comparisons show that the present analysis gives a good agreement with published data.

A further validation is carried out in this study by comparing the results of the present analysis to that obtained by numerically solving the problem under consideration using Darcy–Brinkman–Forchheimer model without radiation effects.

3.1. CFD solution

The problem under consideration is steady, two-dimensional laminar flow through a homogeneous porous matrix and fluid with constant thermo-physical properties. All fluid properties are considered to be constant except for the density in the body force where Boussinesq approximation is used. The governing equations that describe the case are divided into two zones, the clear fluid zone and the porous zone. Therefore, two sets of equations are considered (continuity, momentum and energy equations). A set for clear domain (1) and another set for porous domain (2).

Governing equations. Mass conservation in clear domain (fluid) (1):

$$\frac{\partial u_1}{\partial x} + \frac{\partial v_1}{\partial y} = 0 \quad (20)$$

The momentum equations in the clear domain is

$$\begin{aligned} \rho_f \left(u_1 \frac{\partial u_1}{\partial x} + v_1 \frac{\partial u_1}{\partial y} \right) \\ = -\frac{\partial p_1}{\partial x} + \mu \left(\frac{\partial^2 u_1}{\partial x^2} + \frac{\partial^2 u_1}{\partial y^2} \right) + \rho_f g (T_1 - T_\infty) \end{aligned} \quad (21)$$

$$\begin{aligned} \rho_f \left(u_1 \frac{\partial v_1}{\partial x} + v_1 \frac{\partial v_1}{\partial y} \right) \\ = -\frac{\partial p_1}{\partial y} + \mu \left(\frac{\partial^2 v_1}{\partial x^2} + \frac{\partial^2 v_1}{\partial y^2} \right) + \rho_f g (T_1 - T_\infty) \end{aligned} \quad (22)$$

The energy equation in the clear domain without radiation effect is

$$\rho_f c_p \left(u_1 \frac{\partial T_1}{\partial x} + v_1 \frac{\partial T_1}{\partial y} \right) = k_f \left(\frac{\partial^2 T_1}{\partial x^2} + \frac{\partial^2 T_1}{\partial y^2} \right) \quad (23)$$

Momentum equations in the porous domain (Darcy–Brinkman–Forchheimer equations)

$$\begin{aligned} \rho_f \left(u_2 \frac{\partial u_2}{\partial x} + v_2 \frac{\partial u_2}{\partial y} \right) \\ = -\frac{\partial p_2}{\partial x} + \mu \left(\frac{\partial^2 u_2}{\partial x^2} + \frac{\partial^2 u_2}{\partial y^2} \right) + \rho_f g (T_2 - T_\infty) \\ - \frac{\mu}{K} u_2 - \frac{C_F \rho_f}{\sqrt{K}} \sqrt{u_2^2 + v_2^2} u_2 \end{aligned} \quad (24)$$

$$\begin{aligned} \rho_f \left(u_2 \frac{\partial v_2}{\partial x} + v_2 \frac{\partial v_2}{\partial y} \right) \\ = -\frac{\partial p_2}{\partial y} + \mu \left(\frac{\partial^2 v_2}{\partial x^2} + \frac{\partial^2 v_2}{\partial y^2} \right) + \rho_f g (T_2 - T_\infty) \\ - \frac{\mu}{K} v_2 - \frac{C_F \rho_f}{\sqrt{K}} \sqrt{u_2^2 + v_2^2} v_2 \end{aligned} \quad (25)$$

The energy equation in the porous domain with no radiation effects is

$$\rho_f c_p \left(u_2 \frac{\partial T_2}{\partial x} + v_2 \frac{\partial T_2}{\partial y} \right) = k_{\text{eff}} \left(\frac{\partial^2 T_2}{\partial x^2} + \frac{\partial^2 T_2}{\partial y^2} \right) \quad (26)$$

Since the effect of inertia losses in natural convection flow is small the value of C_F in Eqs. (24), (25) is taken to be zero. Eqs. (20)–(26) are subjected to the following conditions:

- (1) On the vertical surface, $u = v = 0$. At fin base $T_2 = T_b$ and on the rest of the surface $T_1 = T_\infty$. This condition is imposed for comparison purposes to ensure that the heat transfer from the surface takes place through the fin only.
- (2) Far-stream from the surface, following the work of Kuehn and Goldstein [22] and Abu-Hijleh et al. [9], the far-stream boundary condition is divided into an inflow ($\phi < 150^\circ$) and an outflow ($\phi > 150^\circ$) regions, Fig. 2(a). The far-stream temperature boundary conditions are $T_1 = T_\infty$ and $\frac{\partial T_1}{\partial r} = 0$ for the inflow and outflow regions, respectively.
- (3) At the interface between the fin and the clear fluid, the following conditions are applied [8] $u_1 = u_2$, $v_1 = v_2$, $p_1 = p_2$, $T_1 = T_2$, $k_f \frac{\partial T_1}{\partial y} = k_s \frac{\partial T_2}{\partial y}$,

$$\begin{aligned} \mu_f \frac{\partial v_1}{\partial y} = \mu_{\text{eff}} \frac{\partial v_2}{\partial y}, \quad \text{and} \\ \left(\frac{\partial v_1}{\partial x} + \frac{\partial u_1}{\partial y} \right) = \left(\frac{\partial v_2}{\partial x} + \frac{\partial u_2}{\partial y} \right) \end{aligned} \quad (27)$$

Eqs. (20)–(26) along with the relevant boundary conditions are solved using a finite volume solver, Fluent [23]. A simple two-dimensional mesh clustered near walls and at the interface between clear fluid and porous medium is used as shown in Figs. 2(b), 2(c). The pressure field is calculated using the SIMPLE algorithm. The iterative solution is considered to have converged when the maximum values of the normalized absolute residuals across all nodes are less than 10^{-6} .

The far-stream boundary condition placement (R_∞) and the number of grid points in both radial and tangential directions are needed to be predefined for the solution method. Extensive testing was carried out in order to determine the effect of each of these parameters on the solution. This was done to insure that the solution obtained was independent of these predefined parameters. The testing included varying the value of R_∞ from

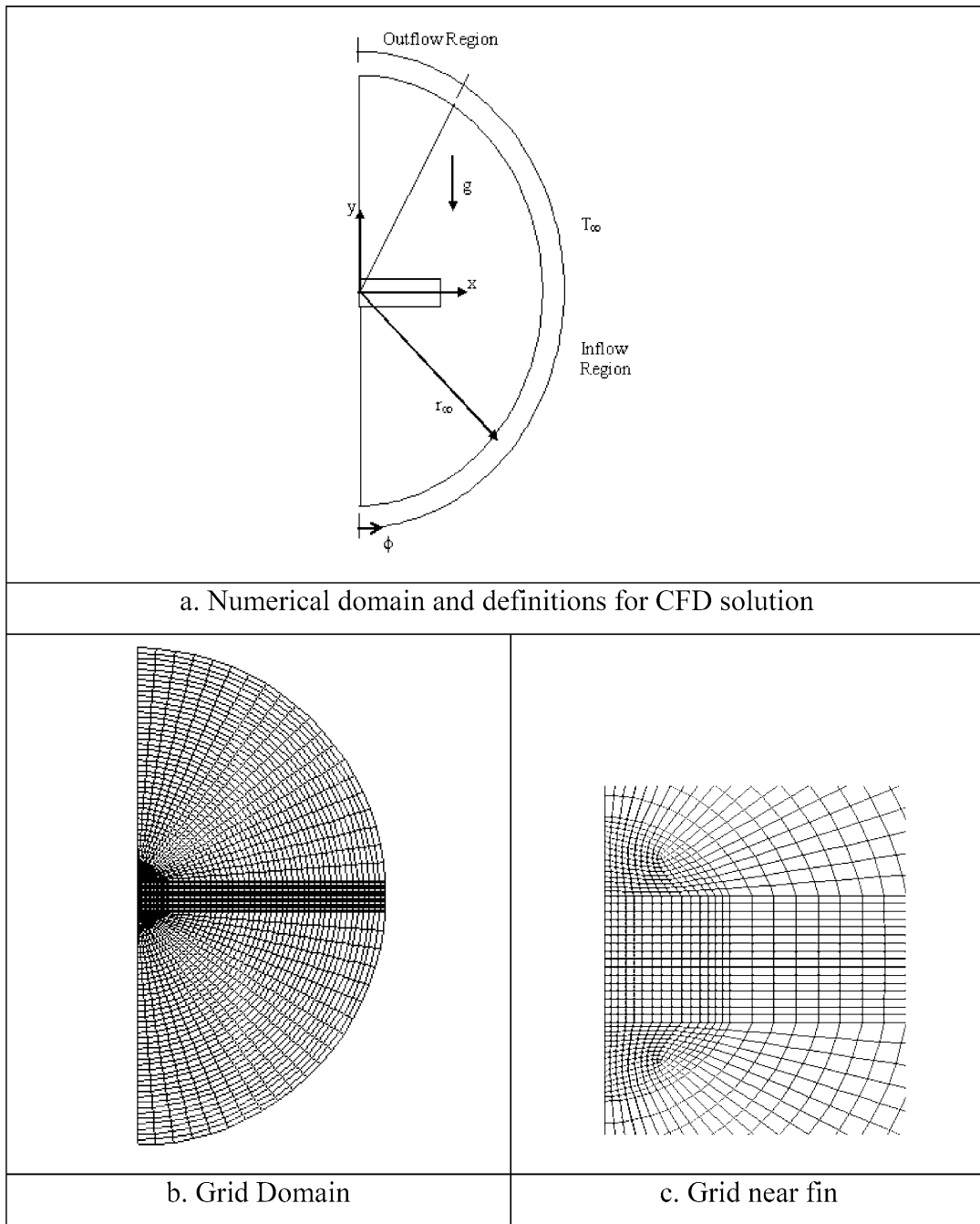


Fig. 2. Grid system for the CFD solution.

10 to 20. For each the value of R_∞ the mesh independent solution was obtained using adaptive grid strategy. A grid of 40 by 80 points in both radial and tangential directions was used as a basic grid. Then, for each case, a number of grid points are added near the regions where the temperature gradient is higher than 0.01.

The values of the average Nusselt number for the case of $Ra^* = 813$, using $R_\infty = 10, 18$ and 20 are $23.59, 23.41, 23.40$, respectively. These numbers indicate that the use of $R_\infty = 18$ is enough to satisfy the boundary condition at far-stream.

Table 1 shows a comparison between the values of average Nusselt number obtained from the solution of Eq. (15) and

that obtained from the CFD solution for an infinitely long fin without radiation effects. It can be seen from this table that the approximate method compares very well with the CFD results.

4. Results and discussion

The numerical results of fin effectiveness parameter are obtained for representative values of the parameters Rd , R_2 and surface temperature parameters θ_b against the Rayleigh numbers Ra^* . It should be noted here that the value of Rd ranges around 0.033 to 0.1 for both CO_2 in the temperature range 38–350 °C and NH_3 vapor in the temperature range 50–205 °C at

Table 1
The average Nusselt number at fin base

Ra^*	\bar{Nu}	\bar{Nu}
	Eq. (15)	CFD
$Rd = R_2 = 0, \tilde{\varepsilon} = 1$		no radiation
	$\theta'(0)$	$\theta'(0)$
54	6.00	6.20
272	13.47	13.20
435	17.04	16.78
474	17.78	18.48
542	19.01	19.61
610	20.17	20.68
678	21.26	21.63
813	23.29	23.41

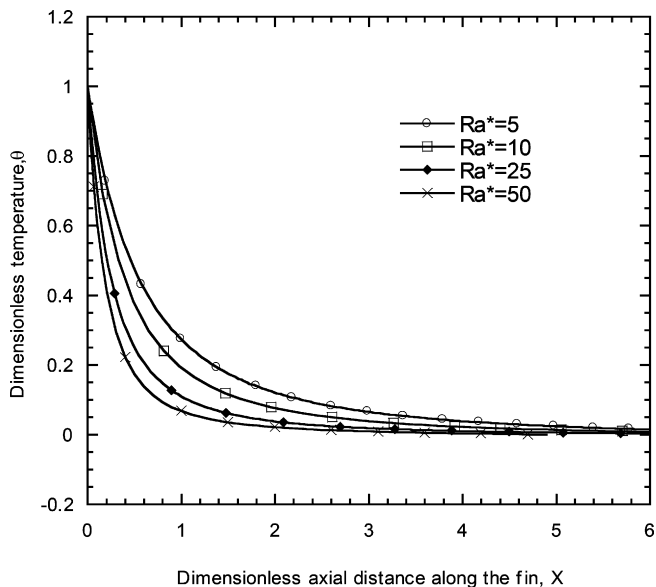


Fig. 3. The distribution of the dimensionless axial temperature along an infinite fin for different Ra^* ($R_2 = 0.01$, $Rd = 0.01$, $W/b = 10$).

1 atm, whereas for water vapor in the temperature range 105–480 °C the Rd values lie between 0.02 and 0.3. Also, it should be noted that for foamed Aluminum porous fins, the value of K is in the range 10^{-6} – 10^{-8} , the porosity is in the range 0.92–0.98 [10], therefore, the surface convection term is small and is neglected.

For practical applications, for example, foamed Aluminum porous fin [10] ($k_s = 200 \text{ W m}^{-1} \text{ K}^{-1}$) of 0.5 porosity filled with a fluid whose properties are $k_s = 0.033 \text{ W m}^{-1} \text{ K}^{-1}$ and $\beta_R = 0.01 \text{ m}^{-1}$ the values of Rd and R_2 are 3.24 and 9.7×10^{-3} , respectively, when the surrounding temperature is at 350 K and black body surfaces. The value of k_{eff} is calculated using the relation $k_{\text{eff}} = \tilde{\varepsilon} k_f + (1 - \tilde{\varepsilon}) k_s$ [6].

The variation of the non-dimensional temperature distribution and its gradient along an infinite fin for different value of Ra^* is shown in Figs. 3 and 4, respectively. It is clear that increasing Ra^* increases the rate of heat removal from the fin and reduces the effective length of the fin. The effect of changing the radiation parameters within the porous fin, i.e., Rd and θ_b , is indicated by Fig. 5. It should be noted that large values of the radiation-conduction parameter, Rd , means that the radia-

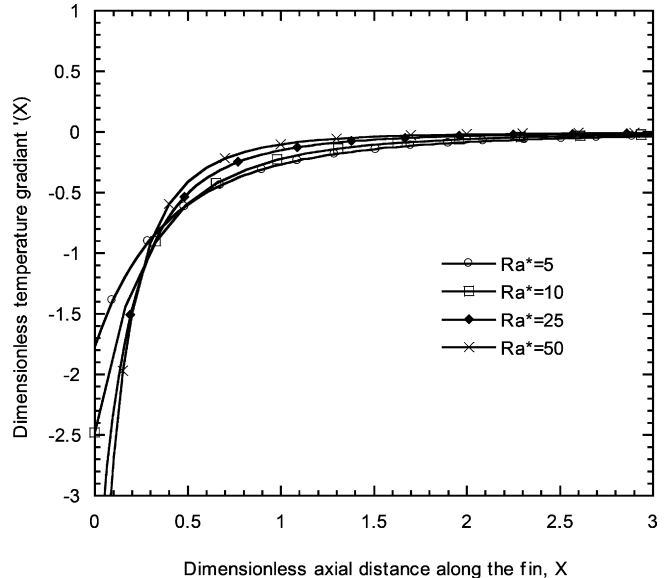


Fig. 4. The distribution of the dimensionless axial temperature along an infinite fin for different Ra^* ($R_2 = 0.01$, $Rd = 0.01$, $W/b = 10$).

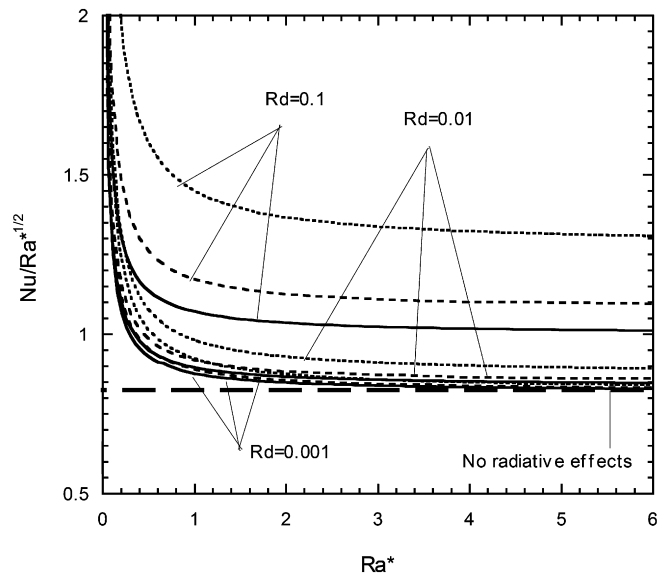


Fig. 5. The variation of $\bar{Nu}/Ra^{*1/2}$ with Ra^* for different Rd and θ_b for infinite fin ($R_2 = 0.01$, $W/b = 10$). (· · · · · $\theta_b = 1.7$, - - - $\theta_b = 1.3$, — $\theta_b = 1.1$).

tion mode dominates and vice versa. As Rd approaches zero the convection mode dominates. On the other hand, when the change in the value of θ_b is independent of the temperature difference between the fin base and the ambient, then the change in θ_b affects only the radiation heat transfer mode (as indicated by Eq. (17)). Several observations can be obtained from this figure: (1) at constant value of Ra^* , the heat transfer from the fin base increases as Rd increases, (2) the radiation losses are important at low Ra^* for all values of Rd and θ_b indicating that the radiation and convection heat transfer are of the same order of magnitude, (3) the effect of radiation on the heat transfer from fin base increases as the value of θ_b increases, and (4) the radiation effect is significant for large values of Rd regardless of the value of Ra^* in the investigated range. In order to

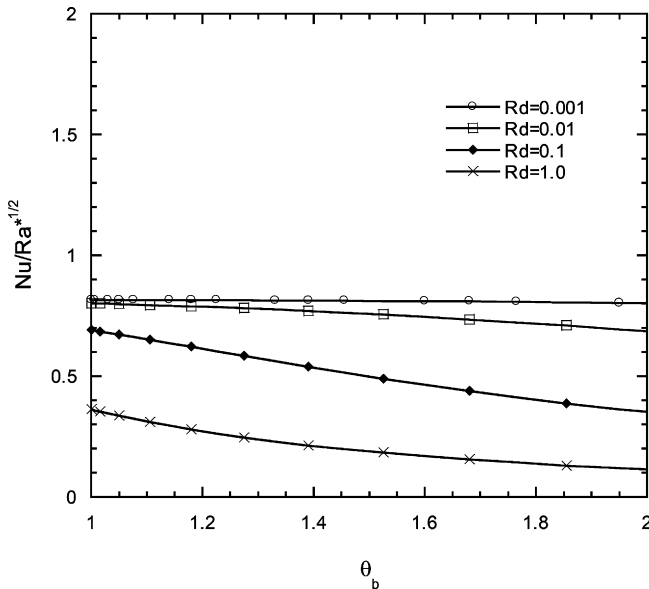


Fig. 6. The variation of $\overline{Nu}/Ra^{*1/2}$ against the variation of θ_b for different values of Rd for insulated tip fin ($R_2 = 0.01$, $X = 10$).

make this result valuable to practical applications, the percentage increase in heat transfer from the fin due to radiation effects is calculated. Thus, when radiation effects are considered with $\theta_b = 1.7$, $Ra^* > 2$, $R_2 = 0.01$ and $W/b = 10$ for infinitely long fin the total heat transfer from fin increases by 7%, 13.7%, and 63% when Rd increases from 0.001, 0.01, and 0.1, respectively. Whereas, when $\theta_b = 1.1$, the total heat transfer from the same fin increases by 3.8%, 6.0%, and 26% when Rd increases from 0.001, 0.01, and 0.1, respectively.

Fig. 6 depicts the effect of Rd and θ_b on the averaged \overline{Nu} (i.e., fin effectiveness, φBi) for an insulated tip fin. At low values of Rd , radiation has almost no effect on the heat transfer from the fin. While at large values of Rd , the heat loss from the fin increases with increasing the value of θ_b .

To investigate the influence of the radiation parameters on the conduction losses and radiation losses, Fig. 7 is displayed. The conduction losses at fin base decreases while radiation losses increase as θ_b increases. Eq. (19) shows that the conduction losses decreases with decreasing $\theta'(0)$ for any value of θ_b , however, the radiation losses depends on both the value $\theta'(0)$ and θ_b . It is clear from Fig. 7 that increasing the value of θ_b increases the radiation losses. That is the effect of increasing radiation losses due to increasing θ_b dominates the effect of reducing the radiation losses due to decreasing $\theta'(0)$. The fact that the convection heat transfer depends on the first power of the temperature difference while the radiation heat transfer depends on the fourth power of the absolute temperatures makes the interaction between these effects is rather complicated. In general, introducing the radiation effects increase the heat transfer from the fin compared with the pure convection case and this increase (enhancement) improves as θ_b increases, as indicated by Fig. 7.

Figs. 8–11 summarize the effect of different parameters on the heat transfer from an insulated tip fin for a range of Ra^* . R_2 represents the parameter that controls the radiation heat trans-

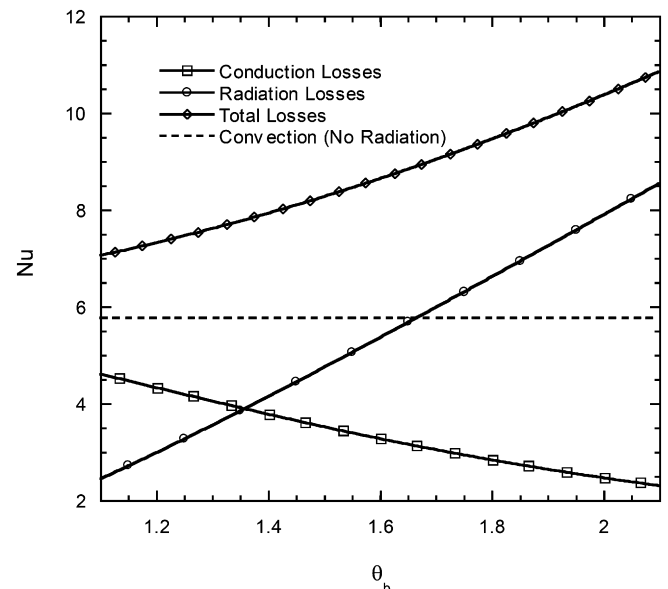


Fig. 7. The effect of changing the surface temperature parameter on conduction and radiation losses for an insulated tip fin ($R_2 = 0.01$, $Rd = 0.1$, $X = 10$, $Ra^* = 50$).

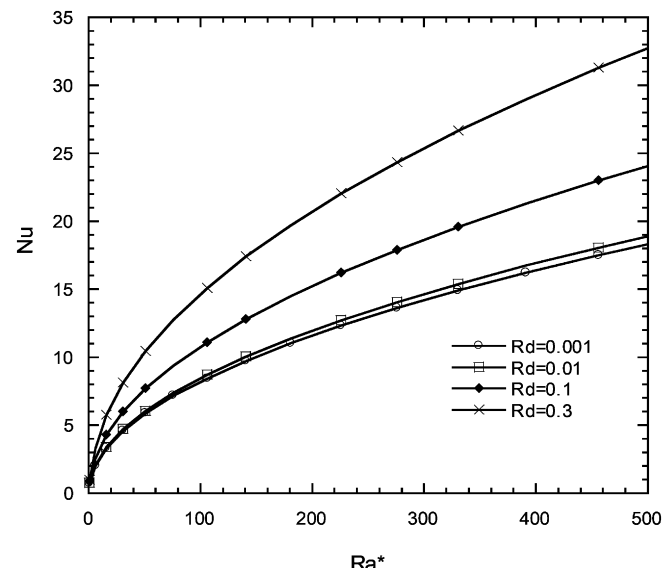


Fig. 8. The variation of \overline{Nu} with the variation of Ra^* at different values of Rd for insulated tip fin ($R_2 = 0.01$, $X = 10$, $\theta_b = 1.3$).

fer between the surface of the fin and the surroundings. These figures indicate that increasing Rd , or R_2 or θ_b result in an increase in the value of \overline{Nu} for any value of Ra^* and that the radiation effect is insignificant compared to the heat convection heat transfer when the values of Rd and R_2 are less than 0.01 and 0.1, respectively. An increase in the value of R_2 for certain T_∞ can be achieved by reducing the effective thermal conductivity of the fin (this can be achieved by increasing fin porosity) or increasing fin length or increasing the emissivity of the fin surface (which is around one for optically thick medium).

Fig. 11 displays the variation of $\overline{Nu}/(Ra^*(1 + 4Rd\theta_b^3))$ with the variation of θ_b . It is clear that as Ra^* increases for fixed value of θ_b , the values of $\overline{Nu}/(Ra^*(1 + 4Rd\theta_b^3))$ reaches an as-

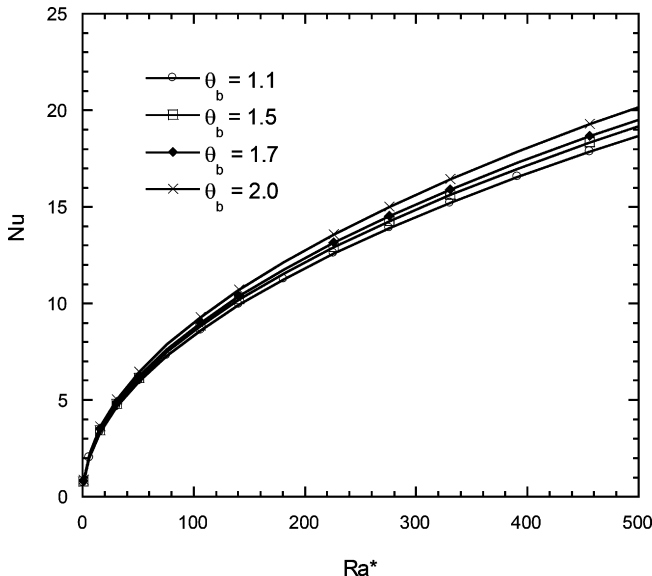


Fig. 9. The variation of \bar{Nu} with the variation of Ra^* at different value of θ_b ($R_2 = 0.1$, $X = 10$, $Rd = 0.3$).

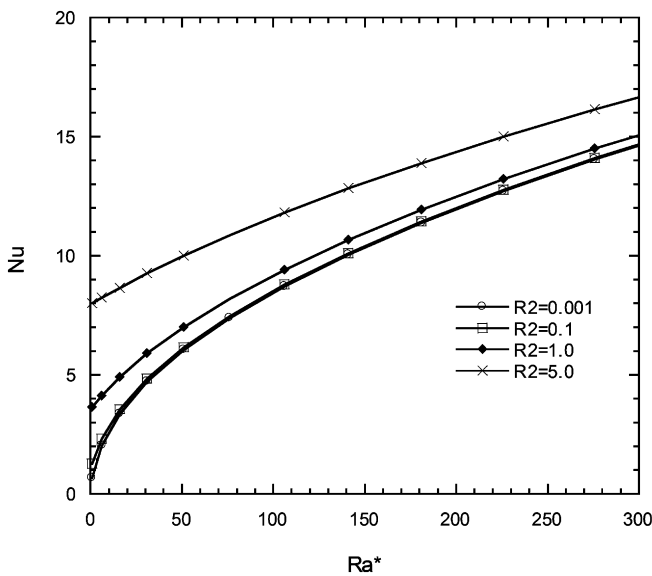


Fig. 10. The effect of the radiation parameter R_2 on \bar{Nu} for insulated tip fin ($X = 10$, $Rd = 0.3$, $\theta_b = 1.3$).

ymptotic value. This asymptotic value depends on the values of θ_b .

5. Conclusions

The problem of laminar natural convection heat transfer from a porous fin attached to vertical surface was studied. The effect of radiation heat transfer was introduced using the Roseland approximation. Simplified assumptions were introduced to the problem resulted in obtaining a closed-form solution for an infinitely long fin with low surface temperature parameter. The closed-form solution and a CFD solution are compared for a case of infinitely long fin without radiation effects and an excellent agreement is obtained. On the other hand, a nonlinear

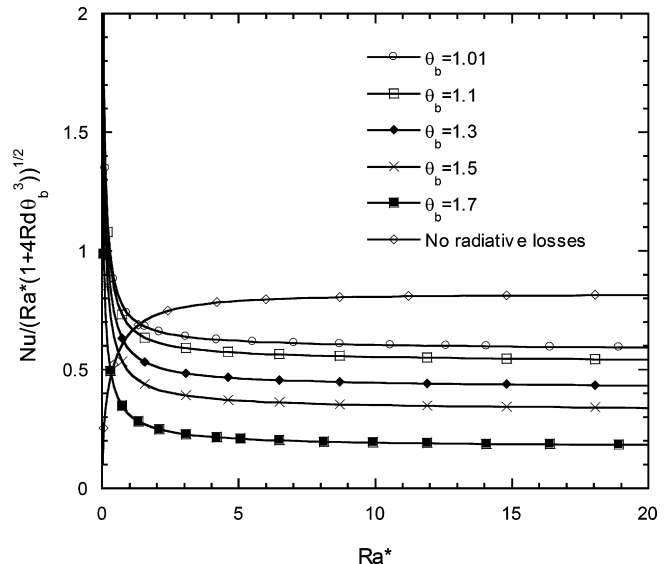


Fig. 11. Effect of radiation parameters Rd and θ_b on the normalized \bar{Nu} for insulated tip fin ($R_2 = 0.01$, $X = 10$, $Rd = 0.3$).

ODE is obtained when the surface temperature parameter, θ_b , is large. The effect of different radiation parameters on \bar{Nu} over a wide range of Ra^* is investigated. In general, including radiation effects increases the heat transfer from the fin, however, these effects are significant at low Ra^* regardless of the values of θ_b and Rd . It is also found that at certain conditions and when $Rd = 1.1$ and $\theta_b = 1.7$ the heat transfer from the fin increases as much as 63% more than the heat transfer from the fin by convection only. It is also found that as Rd or R_2 or θ_b increase, the heat transfer from fin increases.

References

- [1] D. Snider, A. Kraus, The quest for the optimum longitudinal fin profile, ASME HTD 64 (1986) 43–48.
- [2] D. Poulikakos, A. Bejan, Fin geometry for minimum entropy generation in forced convection, ASME J. Heat Transfer 104 (1982) 616–623.
- [3] A.R. Shouman, An exact general solution for the temperature distribution and radiation heat transfer along constant cross-sectional-area fin, Paper No. 67-WA/HT-27, ASME, 1967.
- [4] M. Alkam, M. Al-Nimr, Improving the performance of double-pipe heat exchangers by using porous substrates, Int. J. Heat Mass Transfer 42 (1999) 3609–3618.
- [5] P.C. Huang, K. Vafai, Passive alteration and control of convective heat transfer utilizing alternate porous cavity-block wafers, Int. J. Heat Fluid Flow 15 (1994) 48–61.
- [6] S. Kiwan, M. Al-Nimr, Enhancement of heat transfer using porous fins, ASME J. Heat Transfer 123 (4) (2001) 790–795.
- [7] S. Kiwan, Thermal analysis of natural convection in porous fins, Transport in Porous Media, <http://dx.doi.org/10.1007/s11242-006-0010-3>, 2006.
- [8] S. Kiwan, O. Zeitoun, Natural convection in a horizontal cylindrical annulus using porous fins, Int. J. Numer. Methods, submitted for publication.
- [9] B.A/K. Abu-Hijleh, Natural convection heat transfer from a cylinder with high conductivity permeable fins, ASME J. Heat Transfer 125 (2003) 282–288.
- [10] S.Y. Kim, J.W. Paek, B.H. Kang, Flow and heat transfer correlations for porous fin in a plate-fin heat exchanger, ASME J. Heat Transfer 122 (2000) 572–578.
- [11] M.M. Ali, T.S. Chen, B.F. Armaly, Natural convection–radiation interaction in boundary layer flow over horizontal surface, AIAA J. 22 (1984) 1797–1803.

- [12] M.A. Hossain, H.S. Takhar, Radiation effect on mixed convection along a vertical plate with uniform surface temperature, *Heat Mass Transfer* 31 (1996) 243–248.
- [13] M.A. Hossain, M.A. Alim, Natural convection–radiation interaction on boundary layer flow along a thin vertical cylinder, *Heat Mass Transfer* 32 (1997) 515–520.
- [14] K.A. Yih, Radiation effect on natural convection over a vertical cylinder embedded in a porous media, *Int. Commun. Heat Mass Transfer* 26 (1999) 259–267.
- [15] B. Cherif, M. Sifaoui, Theoretical study of heat transfer by radiation conduction and convection in a semi-transparent porous medium in a cylindrical enclosure, *J. Quant. Spectrosc. Radiat. Transfer* 83 (2004) 519–527.
- [16] I. Badruddin, Z. Zainal, P. Narayana, K. Seetharamu, Heat transfer by radiation and natural convection through a vertical annulus embedded in porous medium, *Int. Commun. Heat Mass Transfer* 33 (4) (2006) 500–507.
- [17] A. Hossain, I. Pop, Radiation effects on free convection over a vertical plate embedded in a porous medium with high porosity, *Int. J. Thermal Sci.* 40 (2001) 289–295.
- [18] R. Siegel, J.R. Howell, *Thermal Radiation Heat Transfer*, third ed., Hemisphere, Washington, DC, 1992 (Chapter 12).
- [19] M.F. Modest, *Radiation Heat Transfer*, McGraw-Hill, USA, 1993 (Chapter 13).
- [20] V. Pereyra, *PASVA3: An Adaptive Finite-Difference FORTRAN Program for First Order Nonlinear Boundary Value Problems*, Lecture Notes in Computer Science, Springer, Berlin, 1978, p. 76.
- [21] A. Bejan, *Convection Heat Transfer*, John Wiley & Sons, New York, 1984 (Chapter 10).
- [22] T.H. Kuehn, R.J. Goldstein, Numerical solutions to the Navier–Stokes equations for laminar natural convection about a horizontal cylinder, *Int. J. Heat Mass Transfer* 23 (1980) 971–979.
- [23] FLUENT (Version 6.1.18), User's Guide, Fluent Inc., 2001.